

Ferromagnetic Superexchange Coupling through a Diamagnetic Iron(II) Ion in a Mixed-Valent Iron(III, II, III) *meso*-Helicate

Toshihide Mochizuki, Takashi Nogami, and Takayuki Ishida*

Department of Applied Physics and Chemistry, The University of Electro-Communications, Chofu, Tokyo 182-8585, Japan

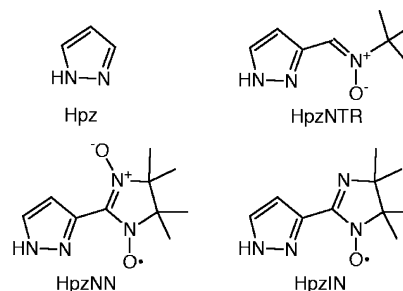
Received October 27, 2008

meso-Helicates $[\text{Ni}_3(\text{pzNTR})_6] \cdot 4\text{CH}_3\text{CN}$ and $[\text{Fe}_3(\text{pzNTR})_6](\text{ClO}_4)_2 \cdot \text{CH}_3\text{OH}$ were prepared (HpzNTR stands for *N*-*tert*-butyl- α -3-pyrazolynitron). The former showed antiferromagnetic coupling between neighboring ions with $J/k_B = -28.2(2)$ K, which can be reasonably interpreted in terms of the superexchange mechanism. On the other hand, the latter exhibited ferromagnetic coupling with $J/k_B = +0.292(8)$ K between the two terminal $S = 5/2$ Fe^{3+} ions through the intervening diamagnetic Fe^{2+} ion. The admixture of low-lying excited states with the ground state stabilizes the ferromagnetically coupled state, like the Prussian blue magnet.

Introduction

Coordination compounds having appreciable magnetic exchange interactions attract much attention for the development of functional magnetic materials.^{1,2} Relatively small π -conjugated bridges are known to be versatile magnetic exchange couplers. We focus our attention to tunable and anionic heteroaromatic ligands such as pyrazolate (pz).³ Actually, we exploited anionic paramagnetic ligands, pzNN and pzIN (see Scheme 1 for the structural formulas), and their oligo- and polymeric supramolecular structures by using Ag^+ .⁴ Furthermore, we applied paramagnetic metal ions and synthesized the trinuclear compounds $[\text{Ni}_3(\text{pzNN})_6]$ and $[\text{Ni}_3(\text{pzIN})_6]$ with a *meso*-helical structure and somewhat complex magnetic interactions.⁵ Thus, our interest lies in the following issues: (1) the establishment of facile synthetic procedures for *meso*-helicates, (2) precise evaluation of each

Scheme 1. Structural Formulas and Abbreviations



magnetic exchange coupling, and (3) development of novel structures of magnetic interest.

A new anionic bridging ligand, pzNTR, from *N*-*tert*-butyl- α -3-pyrazolynitron (HpzNTR) is designed as a diamagnetic version of pzNN and pzIN. Its coordination compounds ($[\text{M}_3(\text{pzNTR})_6]$) will be reported here. The exchange coupling between the Ni^{2+} ions across the pyrazolate was evaluated in $[\text{Ni}_3(\text{pzNTR})_6]$, and furthermore an unexpected magnetic system was characterized in $[\text{Fe}_3(\text{pzNTR})_6]^{2+}$.

Results and Discussion

We prepared $[\text{Ni}_3(\text{pzNTR})_6] \cdot 4\text{CH}_3\text{CN}$ (**1**) from simply mixing $\text{Ni}(\text{NO}_3)_2$ or $\text{Ni}(\text{ClO}_4)_2$ and HpzNTR under basic conditions. The formula was determined by means of elemental analysis and an X-ray crystallographic study. A similar reaction using $\text{Fe}(\text{ClO}_4)_2$ in place of $\text{Ni}(\text{ClO}_4)_2$ did not give $[\text{Fe}_3(\text{pzNTR})_6]$ but mixed-valent $[\text{Fe}_3(\text{pzNTR})_6](\text{ClO}_4)_2 \cdot \text{CH}_3\text{OH}$ (**2**). Autoxidation of Fe^{2+} took place in the presence of air, and Fe^{3+} would be formed in part. Interest-

* To whom correspondence should be addressed. E-mail: ishi@pc.uec.ac.jp.

- (1) Kahn, O. *Molecular Magnetism*; VCH: New York, 1993.
- (2) (a) Iwamura, H.; Inoue, K.; Hayamizu, T. *Pure Appl. Chem.* **1996**, *68*, 243. (b) Kitagawa, S.; Kondo, M. *Bull. Chem. Soc. Jpn.* **1998**, *71*, 1739. (c) Decurtins, S.; Schmalle, H. W.; Schneuwly, P.; Enslin, J.; Gütlich, P. *J. Am. Chem. Soc.* **1994**, *116*, 9521. (d) Coronado, E.; Galan-Mascaros, J. R.; Comez-Garcia, C. J.; Laukhin, V. *Nature* **2000**, *408*, 447. (e) Sato, O. *Acc. Chem. Res.* **2003**, *36*, 692.
- (3) (a) Monica, G. L.; Ardizzoia, G. A. *Prog. Inorg. Chem.* **1997**, *46*, 151. (b) Trofimenko, S. *Prog. Inorg. Chem.* **1986**, *34*, 115. (c) Umakoshi, K.; Yamauchi, Y.; Nakamiya, K.; Kojima, T.; Yamasaki, M.; Kawano, H.; Onishi, M. *Inorg. Chem.* **2003**, *42*, 3907. (d) Angaridis, P. A.; Baran, P.; Boca, R.; Cervantes-Lee, F.; Haase, W.; Mezei, G.; Raptis, R. G.; Werner, R. *Inorg. Chem.* **2002**, *41*, 2219.
- (4) Yamada, S.; Ishida, T.; Nogami, T. *Dalton Trans.* **2004**, 898.
- (5) Yamada, S.; Yasui, M.; Nogami, T.; Ishida, T. *Dalton Trans.* **2006**, 1622.

Table 1. Selected Crystallographic Data for **1** and **2**

compounds	1	2
formula	C ₅₆ H ₈₄ N ₂₂ Ni ₃ O ₆	C ₄₉ H ₇₆ Cl ₂ Fe ₃ N ₁₈ O ₁₅
crystal system	triclinic	monoclinic
space group	<i>P</i> $\bar{1}$	<i>P</i> 2 ₁ / <i>c</i>
<i>a</i> /Å	9.709(2)	11.523(7)
<i>b</i> /Å	13.109(4)	24.015(12)
<i>c</i> /Å	13.984(4)	12.456(7)
α /deg	101.136(5)	90
β /deg	94.915(8)	111.572(7)
γ /deg	98.563(10)	90
<i>V</i> /Å ³	1714.8(8)	3205(3)
<i>Z</i>	1	2
<i>d</i> _{calc} /g cm ⁻³	1.295	1.446
μ (Mo K α)/mm ⁻¹	0.877	0.828
<i>R</i> _{int}	0.059	0.068
<i>R</i> (<i>F</i>) ^a (<i>I</i> > 2 σ (<i>I</i>))	0.0579	0.0466
<i>R</i> _w (<i>F</i> ²) ^b (all data)	0.0892	0.0704
unique reflns	8167	7334
<i>T</i> /K	296	90

$$^a \sum \|F_o\| - |F_c| / \sum \|F_o\|. \quad ^b R_w = [\sum w(F_o^2 - F_c^2)^2 / \sum w(F_o^2)]^{1/2}.$$

ingly, a similar reaction using trivalent Fe(ClO₄)₃ as a starting material afforded the same compound as that with **2**. It may be because the *t*-butylhydroxylamine group formed by the hydrolysis of HpZNTNTR would work as a reducing agent for Fe³⁺. Finally, we prepared **2** by using Fe(ClO₄)₃ and Fe(ClO₄)₂ with a rational molar ratio of 2:1. The preparation of **1** and **2** was highly reproducible, presumably owing to the strong self-assembly nature in this system.

The X-ray crystallographic analysis on **1** and **2** was successfully performed (Table 1). Two molecular structures are quite similar to each other, although the molecular arrangements are completely different because of the presence of counteranions (ClO₄⁻) in **2**. The space groups are *P* $\bar{1}$ and *P*2₁/*c* for **1** and **2**, respectively. We found highly symmetrical [Ni₃(pzNTR)₆]·3CH₃CN in minor crystals as a pseudo-polymorph of **1**. They crystallized in a trigonal *R*3 space group with a genuine 3-fold axis. A sixth of the whole molecule is an independent unit. Unfortunately, the final *R* factors were somewhat large (≥ 0.1).⁶

Figure 1 shows the molecular structures of the [M₃(pzNTR)₆] portions in **1** and **2**. A half of the molecule is crystallographically independent since the inversion center is located at the central metal ion (M1; M = Ni, Fe). Six pz nitrogen atoms are coordinated to octahedral M1. The M1 and M2 ions are triply bridged by the N₂ moiety in pz. The M2 coordination sphere having a screw-type symmetry along the long molecular axis is basically chiral as Δ and Λ (or *P* and *M*) configurations (Figure 1c), but the total molecule has heterochirality owing to the centrosymmetry. Lehn and co-workers exploited various helicates,⁷ and along this line, the present compound is referred to as a *meso*-helicate.⁸

Selected geometrical parameters are summarized in Table 2. The Ni₃pz₆ core in **1** is practically identical to those of

[Ni₃(pzNN)₆] and [Ni₃(pzIN)₆].⁵ The octahedral geometries of Ni1 [2.088(3)–2.122(3) Å for Ni1–N bond lengths] and of Ni2 [2.005(3)–2.017(3) Å for Ni2–N and 2.114(2)–2.129(2) Å for Ni2–O bonds] guarantee their *S*_{Ni} = 1 spin states. The Ni1···Ni2 separation is 3.6631(3) Å in **1**. These distances are comparable with those of the di- and trinuclear nickel(II) compounds triply bridged with triazolates.⁹

In the molecule of **2**, we have to assign the valence (Fe²⁺Fe³⁺₂). The molecular centrosymmetry suggests that the central Fe is divalent. The bond lengths of Fe1–N [1.958(2)–1.970(2) Å] are consistent with the usual bond lengths for low-spin Fe²⁺ ions (*S*_{Fe} = 0).¹⁰ Similarly, those of Fe2–N [2.064(2)–2.073(2) Å] and Fe2–O [2.002(2)–2.020(2) Å] fall in the ordinary bond lengths for high-spin Fe³⁺ ions (*S*_{Fe} = 5/2).¹¹ A relatively “hard” character of Fe³⁺ favors O-ligation. Therefore, we characterized a spin system of [5/2–0–5/2] in the Fe³⁺Fe²⁺Fe³⁺ array. The Fe1···Fe2 separation is 3.7033(4) Å. Several iron(II) compounds involving triple triazolate bridges have been studied from the viewpoint of spin-crossover behavior,^{10,12} but the iron(II) ion in **2** has a low-spin state (*S* = 0) in all temperature regions investigated here, as characterized by means of X-ray diffraction as well as magnetic studies (see below).

The spin quantities and their magnetic couplings were studied on a SQUID magnetometer. Figure 2 shows the temperature dependence of the products, $\chi_m T$, for polycrystalline specimens of **1** and **2**, where χ_m is the molar magnetic susceptibility on the trinuclear molecule basis.

The $\chi_m T$ value of **1** was 2.99 cm³ K mol⁻¹ at 300 K, which is close to the spin-only value of 3.0 cm³ K mol⁻¹ of the species having three *S*_{Ni} = 1 centers. On cooling, the $\chi_m T$ value monotonically decreased and showed a plateau, clearly indicating the residual *S*_{total} = 1 quantity owing to considerably strong antiferromagnetic coupling.

To estimate the magnitude of the magnetic couplings of **1**, we utilized the Heisenberg spin Hamiltonian $H = -2J(S_1 \cdot S_2 + S_2 \cdot S_3)$ (the inset of Figure 2) for the Ni₃ core.¹³ The best fit to the van Vleck equation (eq 1),

$$\chi_m = \frac{2Ng^2\mu_B^2}{k_B T} \frac{14 + 5e^{-2x} + e^{-4x} + 6e^{-6x} + e^{-10x}}{7 + 5e^{-2x} + 3e^{-4x} + 8e^{-6x} + e^{-8x} + 3e^{-10x}} \quad (1)$$

where $x = -J/k_B T$, gave the optimized parameters $J/k_B = -28.2(2)$ K and $g = 2.178(2)$. The calculated curve well-reproduced the experimental data (Figure 2). There seem to be other effects, such as zero-field splitting and intermolecular magnetic interactions, leading to the tiny final drop

(9) Ding, B.; Yi, L.; Shen, W.-Z.; Cheng, P.; Liao, D.-Z.; Yan, S.-P.; Jiang, Z.-H. *J. Mol. Struct.* **2006**, *784*, 138.

(10) (a) Gütllich, P.; Goodwin, H. A. *Spin Crossover in Transition Metal Compounds I, II, and III*; Springer-Verlag: Berlin, 2004. (b) Garcia, Y.; Guionneau, P.; Bravic, G.; Chasseau, D.; Howard, J. A. K.; Kahn, O.; Ksenofontov, V.; Reiman, S.; Gütllich, P. *Eur. J. Inorg. Chem.* **2000**, 1531. (c) Gallois, B.; Real, J.-A.; Hauw, C.; Zarembowitch, J. *Inorg. Chem.* **1990**, *29*, 1152. (d) Oso, Y.; Kanatsuki, D.; Saito, S.; Nogami, T.; Ishida, T. *Chem. Lett.* **2008**, *37*, 760.

(11) (a) Conti, A. J.; Chadha, R. K.; Sena, K. M.; Rheingold, A. L.; Hendrickson, D. N. *Inorg. Chem.* **1993**, *32*, 2670. (b) Hayami, S.; Matoba, T.; Nomiyama, S.; Kojima, T.; Osaki, S.; Maeda, Y. *Bull. Chem. Soc. Jpn.* **1997**, *70*, 3001.

(6) Furthermore, we found a highly symmetrical cobalt(II) analogue, [Co₃(pzNTR)₆], which crystallized in a cubic *Pa*3 space group. The structure and magnetic properties will be reported in a due course.

(7) (a) Lehn, J.-M. *Angew. Chem., Int. Ed. Engl.* **1990**, *29*, 1304. (b) Lehn, J.-M. *Supramolecular Chemistry*; VCH: New York, 1995; Chapter 9. (c) Krämer, R.; Lehn, J.-M.; Marquis-Rigault, A. *Proc. Natl. Acad. Sci. U. S. A.* **1993**, *90*, 5394.

(8) (a) Albrecht, M. *Chem.—Eur. J.* **2000**, *6*, 3485. (b) Caulder, D. L.; Raymond, K. N. *J. Chem. Soc., Dalton Trans.* **1999**, 1185.

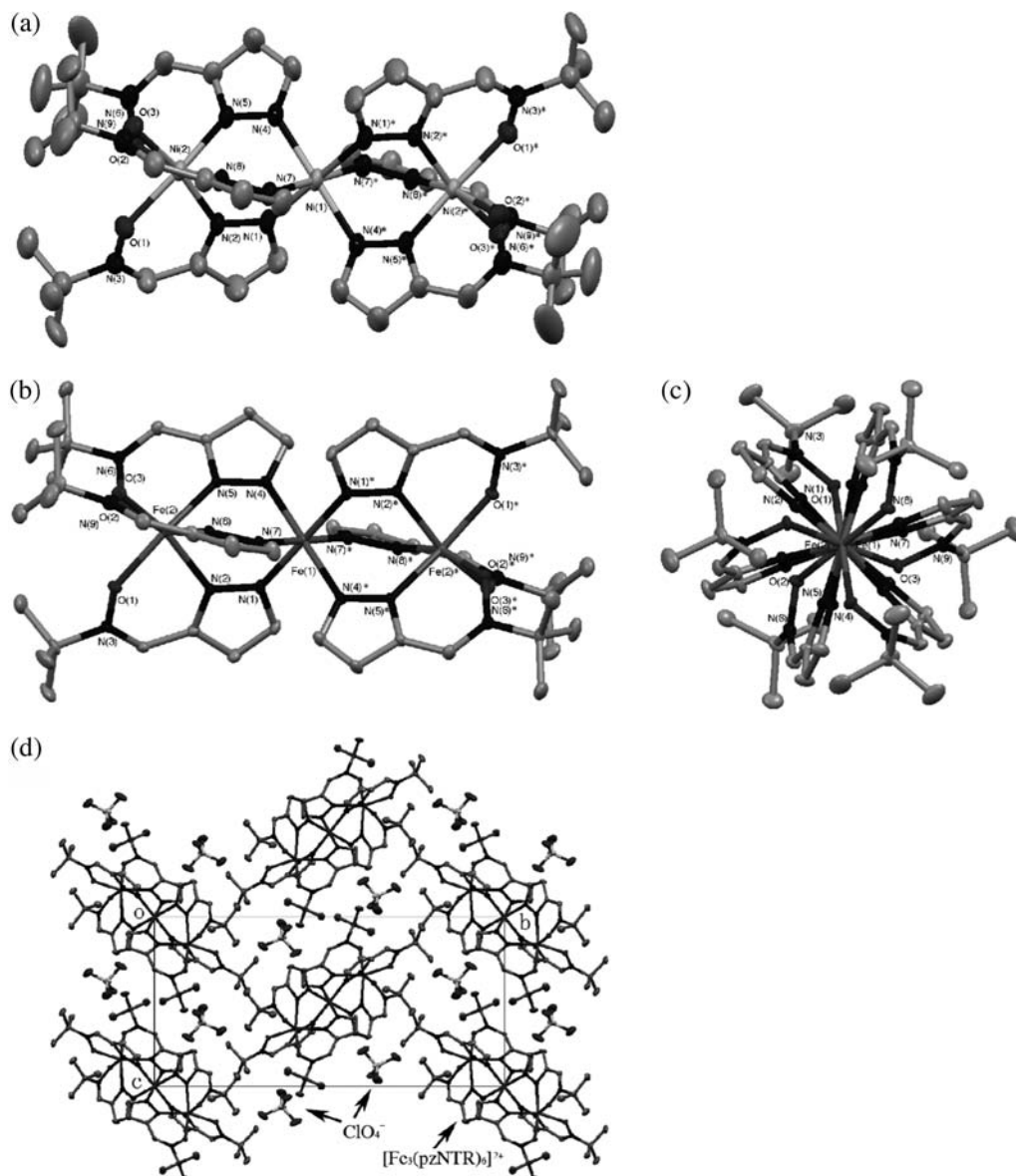


Figure 1. (a) Molecular structure of $[\text{Ni}_3(\text{pzNTR})_6]$ in **1**. Symmetry operation code of * is $-x, -y, -z$. (b) Side and (c) top views of $[\text{Fe}_3(\text{pzNTR})_6]^{2+}$ in **2**. Symmetry operation code of * is $2-x, -y, -z$. Thermal ellipsoids are drawn at the 50% probability level. Selected atoms are numbered. Hydrogen atoms are omitted. (d) Molecular arrangement of **2** viewed along the a axis. Six formula units are shown.

Table 2. Selected Bond Lengths (Å) and Angles for **1** and **2**

compounds	1 (M = Ni)	2 (M = Fe)
M1–N1	2.122(3)	1.958(2)
M1–N4	2.088(3)	1.961(2)
M1–N7	2.103(3)	1.970(2)
M2–N2	2.005(3)	2.072(2)
M2–N5	2.017(3)	2.073(2)
M2–N8	2.013(2)	2.064(2)
M2–O1	2.129(2)	2.002(2)
M2–O2	2.114(2)	2.012(2)
M2–O3	2.118(2)	2.020(2)
N1–M1–N4	90.96(12)	90.63(10)
N1–M1–N7	90.10(12)	91.36(10)
N4–M1–N7	88.40(12)	91.31(9)
N2–M2–N5	92.16(12)	86.93(9)
N2–M2–N8	91.45(12)	87.01(9)
N5–M2–N8	90.87(12)	87.51(9)
O1–M2–N2	84.25(11)	82.16(9)
O2–M2–N5	83.39(10)	81.79(9)
O3–M2–N8	83.61(11)	81.63(9)

of $\chi_m T$. The intermolecular interaction is practically negligible in the present system. The ground $S = 1$ state of **1**

was confirmed from the $M-H$ measurement (Figure 3a). The experimental curve measured at 2.2 K obeyed the Brillouin function with $S = 1$.

Thanks to masking the paramagnetic properties from six ligands in $[\text{Ni}_3(\text{pzNN}_6)]$ and $[\text{Ni}_3(\text{pzIN}_6)]$,⁵ we precisely determined the $\text{Ni}\cdots\text{Ni}$ exchange coupling. The magnetic properties of doubly pz-bridged dinuclear Ni^{2+} complexes have been studied,¹⁴ and the present value was close to the

(12) Shakirova, O. G.; Lavrenova, L. G.; Shvedenkov, Y. G.; Berezovskii, G. A.; Naumov, D. Y.; Sheludyakova, L. A.; Dolgushin, G. V.; Larionov, S. V. *Russ J. Coord. Chem.* **2004**, *30*, 473. translated from *Koord. Khim.* **2004**, *30*, 507.

(13) Ginsberg, A. P.; Martin, R. L.; Sherwood, R. C. *Inorg. Chem.* **1968**, *7*, 932.

(14) (a) Röder, J. C.; Meyer, F.; Kaifer, E.; Pritzkow, H. *Eur. J. Inorg. Chem.* **2004**, 1646. (b) Krämer, R.; Fritsky, I. O.; Pritzkow, H.; Kovbasyuk, L. A. *J. Chem. Soc., Dalton Trans.* **2002**, 1307.

(15) (a) Anderson, P. W. *Phys. Rev.* **1959**, *115*, 2. (b) Goodenough, J. B. *Phys. Rev.* **1955**, *100*, 564. (c) Kanamori, J. *J. Phys. Chem. Solids* **1959**, *10*, 87. (d) Escure, A.; Vicente, R.; Mernari, B.; El Gueddi, A.; Pierrot, M. *Inorg. Chem.* **1997**, *36*, 2511.

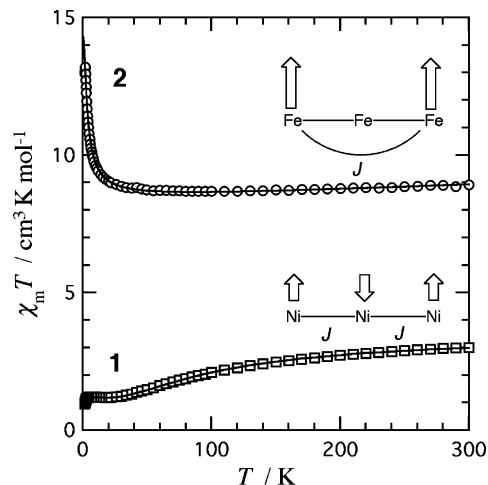


Figure 2. Temperature dependence of $\chi_m T$ for **1** and **2** measured with applied fields of 5000 and 500 Oe, respectively. The solid lines represent calculated curves. For the equation and parameters, see the text. Exchange coupling models are also shown in the insets. The ground-state spin structures are depicted with arrows.

typical reported ones. These antiferromagnetic couplings can be reasonably accounted for in terms of the superexchange mechanism.^{15,16}

Pyrazolate bridges usually work as an antiferromagnetic coupler, and the following result seems to be quite exceptional. The $\chi_m T$ value of **2** was $8.91 \text{ cm}^3 \text{ K mol}^{-1}$ at 300 K, consistent with the entity of two $S_{\text{Fe}} = 5/2$ spins; the spin-only value is $8.75 \text{ cm}^3 \text{ K mol}^{-1}$. A sharp increase on cooling is simply explained as the presence of ferromagnetic coupling. A very slight increase on heating to 300 K is attributed to a contribution of temperature-independent paramagnetism. To estimate the magnitude of the magnetic couplings in **2**, we applied the Heisenberg spin Hamiltonian $H = -JS_1 \cdot S_3$ for the terminal $S_{\text{Fe}} = 5/2$ spin sources,¹⁶ giving the following equation modified with a χ_{TIP} term (eq 2):

$$\chi_m = \frac{2Ng^2\mu_B^2}{k_B T} \frac{e^{-2x} + 5e^{-6x} + 14e^{-12x} + 30e^{-20x} + 55e^{-30x}}{1 + 3e^{-2x} + 5e^{-6x} + 7e^{-12x} + 9e^{-20x} + 11e^{-30x}} + \chi_{\text{TIP}} \quad (2)$$

where $x = -J/k_B T$. The parameters were optimized as $J/k_B = +0.292(8) \text{ K}$ and $g = 1.951(4)$ with $\chi_{\text{TIP}} = 0.00093(11) \text{ cm}^3 \text{ mol}^{-1}$.¹⁷ The g value was independently determined from the powder X-band electron paramagnetic resonance (EPR) measurements. A broad line appeared at $g_{\text{iso}} = 1.9982$ with $\Delta H_{\text{p-p}} = 127 \text{ mT}$ for a polycrystalline specimen of **2**.¹⁸

Additional evidence for the ferromagnetic coupling was obtained from the magnetization curve. We measured the

magnetization of polycrystalline **2** at 2.2 K and found that the curve exceeded the theoretical Brillouin function of $S = 5/2$ (Figure 3b). However, the appreciable swelling was found only below 2 T. On further applying the magnetic field, a contribution of slowly saturated magnetization seems to be superposed, and the total magnetization curve did not obey any Brillouin function. A possible reason is as follows. The molecules of **2** are arranged in a zigzag manner in a monoclinic cell, as described in Figure 1d, and accordingly the easy axes of the neighboring molecules are canted toward each other, leading to a delayed macroscopic saturation due to the orientation of each moment.

We have to discuss how the two $S_{\text{Fe}} = 5/2$ spins are correlated ferromagnetically in **2**. The long $\text{Fe}2 \cdots \text{Fe}2^*$ distance of $7.4065(6) \text{ \AA}$ excludes a possibility of direct through-space contribution. This distance is longer than those of $\text{Ag}(\text{CN})_2^-$ ¹⁹ and $\text{Ni}(\text{CN})_4^{2-}$ bridges²⁰ reported to behave as superexchange couplers. The admixture mechanism seems responsible for the sizable coupling observed in **2**. Superexchange between two high-spin d^5 spins across a low-spin d^6 ion can be proposed, as schematically drawn in Figure 4, like the Prussian blue magnet.²¹ Namely, the admixture of low-lying excited states with the ground state stabilizes the ferromagnetically coupled state with $S_{\text{total}} = 5$. There are two ways of charge transfer (CT), or delocalization, available to imagine an excited state. While a CT from Fe^{2+} to Fe^{3+} ions (a) seems likely from their nominal charges, a CT from Fe^{3+} to Fe^{2+} ions (b) is favorable for the σ pathway involving the nitrogen lone pairs. The vis-NIR absorption spectrum of **2** in Nujol exhibited a broad maximum at ca. 1200 nm, probably ascribable to an intervalence CT band. Compound **2** belongs to class II rather than III according to the Robin-Day classification.²²

The exchange parameter of **2** ($J/k_B = +0.292(8) \text{ K}$) is much larger than that of Prussian blue ($J/k_B = \text{ca. } 0.053 \text{ K}$) estimated from the mean-field approximation, $\theta = 2zJS(S+1)/3k_B$ with $\theta \approx T_C = 5.6 \text{ K}$ ²³ and $z = 18$; even $z = 6$ would give J/k_B as small as 0.16 K). The $\text{Fe}^{3+} \cdots \text{Fe}^{3+}$ distance of **2** is shorter than that of the Prussian blue (10.28 \AA ²³), and the triply bridged structure transmits the $\text{Fe}^{3+} \cdots \text{Fe}^{3+}$ exchange, probably bringing about the stronger ferromagnetic coupling in **2**. Fukita et al. previously reported three-dimensional bimetallic assemblies of the general formula $[\text{Ni}^{\text{II}}(\text{L})_2]_3[\text{Fe}^{\text{II}}(\text{CN})_6]\text{X}_2$ ($\text{L} = \text{en}$ etc.), which exhibited ferromagnetic exchange couplings between the nearest nick-

(16) Ishida, T.; Kawakami, T.; Mitsubori, S.-i.; Nogami, T.; Yamaguchi, K.; Iwamura, H. *J. Chem. Soc., Dalton Trans.* **2002**, 3177.

(17) The temperature-independent paramagnetism for iron(III) has been reported typically as ca. $300 \times 10^{-6} \text{ cm}^3 \text{ mol}^{-1}$ per ion. See: (a) Albel, B.; Bill, E.; Brosch, O.; Weyhermüller, T.; Wieghart, K. *Eur. J. Inorg. Chem.* **2000**, 139. (b) Hibbs, W.; van Koningsbruggen, P. J.; Arif, A. M.; Shum, W. W.; Miller, J. S. *Inorg. Chem.* **2003**, 42, 5645. (c) Tanase, S.; Bouwman, E.; Long, G. J.; Shahin, A. M.; de Gelder, R.; Mills, A. M.; Spek, A. L.; Reedijk, J. *Polyhedron* **2005**, 24, 41.

(18) The error in the g factor may be attributed to the purity of the specimen (95.3%) or the ratio of the solvated methanol molecules in the crystal. See the Experimental Section.

(19) Panja, A.; Shaikh, N.; Vojtisek, P.; Gao, S.; Banerjee, P. *New J. Chem.* **2002**, 26, 1025.

(20) (a) Smékal, Z.; Travnicek, Z.; Mrozinski, J.; Marek, J. *Inorg. Chem. Commun.* **2003**, 6, 1395. (b) Kou, H.-Z.; Si, S.-F.; Gao, S.; Liao, D.-Z.; Jiang, Z.-H.; Yan, S.-P.; Fan, Y.-G.; Wang, G.-L. *Eur. J. Inorg. Chem.* **2002**, 699.

(21) (a) Verdager, M.; Girolami, G. In *Magnetism: Molecule to Materials V*; Miller, J. S., Drillon, M., Eds.; Wiley-VCH: Weinheim, Germany, 2004. (b) Mayoh, B.; Day, P. *J. Chem. Soc., Dalton Trans.* **1976**, 1483. (c) Mayoh, B.; Day, P. *J. Chem. Soc., Dalton Trans.* **1974**, 896. (d) Rogez, G.; Marvilliers, A.; Riviere, E.; Audiere, J.-P.; Lloret, F.; Verret, F.; Goujon, A.; Mendenez, N.; Girerd, J.-J.; Mallah, T. *Angew. Chem., Int. Ed.* **2000**, 39, 2885.

(22) Robin, M. B.; Day, P. *Adv. Inorg. Chem. Radiochem.* **1967**, 10, 247.

(23) Herren, F.; Fischer, P.; Ludi, A.; Halg, W. *Inorg. Chem.* **1980**, 19, 956.

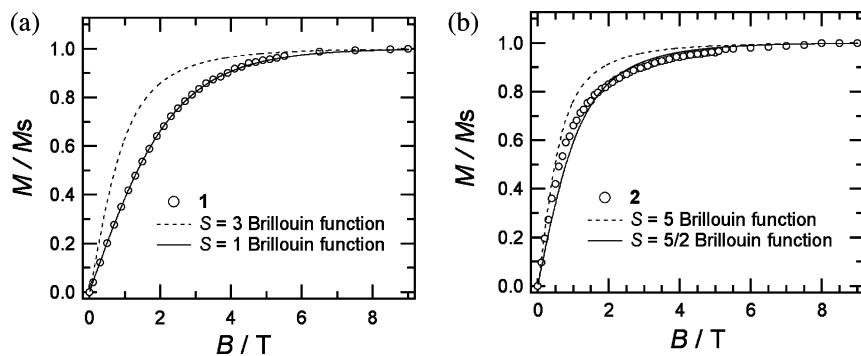


Figure 3. Magnetization curves for **1** (a) and **2** (b) measured at 2.2 K. The solid and dotted lines represent the Brillouin functions.

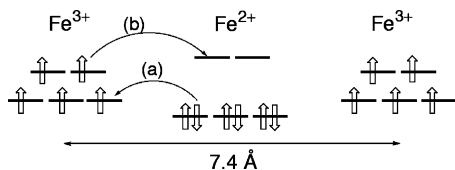


Figure 4. Superexchange mechanism between two high-spin Fe^{3+} ions across a low-spin Fe^{2+} ion, based on electron transfers (a) from d^6 to d^5 ions and (b) from d^5 to d^6 ions.

el(II) ($S = 1$) ions through a diamagnetic Fe^{2+} ion.²⁴ This report supports the admixture mechanism presented here, but the magnitudes of their couplings were much smaller than that of **2**. In addition, a vast number of cyanide-bridged coordination compounds have been known and intensively investigated to date, and the present compound seems to have an advantage for the absence of toxic cyanide anions.

Conclusion

The strong self-assembled nature of pzNTR, as well as pzNN and pzIN, can be pointed out because of high reproducibility using various 3d-metal ions and reaction conditions. We have established the synthetic procedure using pzNTR for *meso*-helicates, precisely evaluated magnetic exchange coupling in the nickel and iron compounds, and developed the novel trinuclear iron compound showing ferromagnetic coupling. Owing to the small and discrete system, the magnetic couplings can be well defined, and the magnetic exchange parameter has been precisely determined. The iron derivative is regarded as an easily available prototype for a Prussian-blue-type exchange mechanism.

Experimental Section

Caution! Perchlorate salts should be handled with a great care.

Preparation of *N*-tert-Butyl- α -3-pyrazolylnitron. A new pyrazolyl ligand, *N*-tert-butyl- α -3-pyrazolylnitron (HpzNTR), was prepared according to the condensation method reported for an *N*-tert-butyl- α -1,2,4-triazol-3-ylnitron derivative.²⁵ A mixture containing 3-formylpyrazole (Merck; 0.98 g; 0.010 mol) and tert-butylhydroxylamine (0.89 g; 0.010 mol) in chloroform (20 mL) was stirred at room temperature for 4 h. The mixture was dried over anhydrous MgSO_4 , concentrated under reduced pressure, and passed through a silica-gel column eluted with ethyl acetate, giving HpzNTR (0.41 g; 2.5 mmol; 25%) as yellow solids. Mp.: 118–119

$^\circ\text{C}$. ^1H NMR (270 MHz, CDCl_3): δ 7.96 (s, 1H), 7.64 (s, 1H), 6.53 (s, 1H), 1.22 (s, 9H). ^{13}C NMR (68 MHz, CDCl_3): δ 28.0, 70.2, 107.0, 120.3, 134.8, 139.1. MS (ESI, methanol): m/z 357.1 ($\text{M}_2 + \text{Li}^+$), 373.1 ($\text{M}_2 + \text{Na}^+$). IR (KBr disk): 3150, 1605, 1506, 1479, 1355, 847 cm^{-1} . 3-Formylpyrazole can also be prepared according to the method reported for 4-formylpyrimidine²⁶ with a modification, as follows. The condensation of *N,N*-dimethylformamide diethyl acetal and pyruvic aldehyde dimethyl acetal gave 4-(*N,N*-dimethylamino)-1,1-dimethoxy-3-buten-2-one, which was successively treated with hydrazine monohydrate. The dimethyl acetal of 3-formylpyrazole was deprotected with sulfuric acid and gave an unprotected compound.

Preparation of $[\text{Ni}_3(\text{pzNTR})_6] \cdot 4\text{CH}_3\text{CN}$ (1**).** Complexation was carried out in an acetonitrile solution (1 mL) containing HpzNTR (50 mg; 0.30 mmol) and $\text{Ni}(\text{NO}_3)_2 \cdot 6\text{H}_2\text{O}$ (44 mg; 0.150 mmol) in the presence of 1,8-diazabicyclo[5.4.0]undec-7-ene (DBU; 45 mg; 0.30 mmol). After the resultant clear dark green solution was allowed to stand in a refrigerator for a week, dark green plate crystals of $[\text{Ni}_3(\text{pzNTR})_6]$ were precipitated and separated by filtration. The yield of **1** was 9.8 mg (17%). Mp.: >300 $^\circ\text{C}$ (dec.). The crystals were suitable for X-ray diffraction and magnetic studies without further purification. The elemental analysis (C, H, N) supported their chemical composition with a 1:2 metal/ligand ratio and the presence of four solvated acetonitrile molecules. Anal. calcd for $\text{C}_{56}\text{H}_{84}\text{N}_{22}\text{Ni}_3\text{O}_6$ (**1**): C, 50.29; H, 6.33; N, 23.04%. Found: C, 50.77; H, 6.80; N, 23.02%. IR (KBr disk): 2977, 2249, 1612, 1377 cm^{-1} . MS (ESI, 1/3 *N,N*-dimethylformamide/methanol): m/z 1006.1 ($[\text{Ni}_3(\text{pzNTR})_5]^+$), 614.0 ($[\text{Ni}_2(\text{pzNTR})_3]^+$).

When we utilized 54.85 mg (0.15mmol) of $\text{Ni}(\text{ClO}_4)_2 \cdot 6\text{H}_2\text{O}$ in place of $\text{Ni}(\text{NO}_3)_2 \cdot 6\text{H}_2\text{O}$, a similar procedure gave dark green plate crystals of $[\text{Ni}_3(\text{pzNTR})_6]$ (13.9 mg; 24%).

Preparation of $[\text{Fe}_3(\text{pzNTR})_6](\text{ClO}_4)_2 \cdot \text{CH}_3\text{OH}$ (2**).** Following methods A, B, and C gave the identical compound $[\text{Fe}_3(\text{pzNTR})_6](\text{ClO}_4)_2 \cdot \text{CH}_3\text{OH}$, which is confirmed by means of X-ray diffraction and magnetic studies and elemental analysis.

Method A. A methanol solution (2 mL) containing $\text{Fe}(\text{ClO}_4)_2 \cdot 6\text{H}_2\text{O}$ (36 mg; 0.10 mmol) was added to a methanol solution (2 mL) containing HpzNTR (33 mg; 0.20 mmol), and successively DBU (30 mg; 0.20 mmol) was added dropwise to the mixture. The resultant solution turned black and was allowed to stand at room temperature for 1 day. Black crystals of $[\text{Fe}_3(\text{pzNTR})_6](\text{ClO}_4)_2 \cdot \text{CH}_3\text{OH}$ (31 mg) were precipitated and separated on a filter in 23% yield.

Method B. A method similar to method A using a methanol solution (1 mL) of $\text{Fe}(\text{ClO}_4)_3 \cdot 6\text{H}_2\text{O}$ (36 mg; 0.10 mmol), a

(24) Fukita, N.; Ohba, M.; Okawa, H.; Matsuda, K.; Iwamura, H. *Inorg. Chem.* **1998**, *37*, 842.

(25) Sutter, J.-P.; Kahn, M.; Kahn, O. *Adv. Mater.* **1999**, *11*, 863.

(26) Omata, J.; Ishida, T.; Hashizume, D.; Iwasaki, F.; Nogami, T. *Inorg. Chem.* **2001**, *40*, 3954.

dichloromethane solution (1 mL) of HPzNTR (33 mg; 0.20 mmol), and DBU (30 mg; 0.20 mmol) gave black crystals of $[\text{Fe}_3(\text{pzNTR})_6](\text{ClO}_4)_2 \cdot \text{CH}_3\text{OH}$ (16 mg) in 12% yield.

Method C. A methanol solution (3 mL) containing $\text{Fe}(\text{ClO}_4)_3 \cdot 6\text{H}_2\text{O}$ (31 mg; 0.067 mmol) and $\text{Fe}(\text{ClO}_4)_2 \cdot 6\text{H}_2\text{O}$ (12 mg; 0.033 mmol) was added to a methanol solution (1 mL) containing HPzNTR (33 mg; 0.20 mmol), and successively DBU (30 mg; 0.20 mmol) was added dropwise to the mixture. After being allowed to stand at room temperature for 1 day, black crystals of $[\text{Fe}_3(\text{pzNTR})_6](\text{ClO}_4)_2 \cdot \text{CH}_3\text{OH}$ (28 mg) were precipitated and separated on a filter in 20% yield.

Complex 2. Mp.: >300 °C (dec). Anal. calcd for $\text{C}_{48.5}\text{H}_{74}\text{Cl}_2\text{-Fe}_3\text{N}_{18}\text{O}_{14.5}$ ($[\text{Fe}_3(\text{pzNTR})_6](\text{ClO}_4)_2 \cdot 0.5\text{CH}_3\text{OH}$): C, 42.22%; H, 5.41%; N, 18.27%. Found: C, 41.97%; H, 5.44%; N, 18.21%. IR (KBr disk): 3434, 1616, 1380 cm^{-1} . The ratio of solvated methanol molecules depended on preparation batches. Typically, n in $[\text{Fe}_3(\text{pzNTR})_6](\text{ClO}_4)_2 \cdot n\text{CH}_3\text{OH}$ varied 0.5–1.0 in the elemental analysis owing to the partial liberation of methanol, and the crystal structure analysis at 90 K indicates that n is close to 1.

X-Ray Crystallographic Analysis. X-ray diffraction data of **1** and **2** were collected on Rigaku R-axis RAPID and Saturn70 CCD diffractometers, respectively, with graphite monochromated Mo $K\alpha$ ($\lambda = 0.71069$ Å) radiation. The structures were directly solved, and the parameters were refined in the CrystalStructure program package.²⁷ Numerical absorption correction was used. The thermal displacement parameters of non-hydrogen atoms were refined anisotropically. The hydrogen atoms were placed at calculated positions, and their parameters were refined as “riding.”

(27) *Crystal Structure*, version 3.8.2; Rigaku and Rigaku/MSK: The Woodlands, TX, 2000–2006.

Magnetic Measurements. Magnetic susceptibilities of the polycrystalline samples of **1** and **2** were measured on a Quantum Design MPMS SQUID magnetometer at applied magnetic fields of 5000 and 500 Oe, respectively, in a temperature range 1.8–300 K. Magnetization curves of **1** and **2** were recorded on a Quantum Design PPMS apparatus equipped with an ac/dc magnetization probe, and the magnetic field was applied up to 90000 Oe at 2.2 K. The magnetic response was corrected with diamagnetic blank data of the sample holder obtained separately. The diamagnetic contribution of the sample itself was estimated from Pascal's constant.

EPR Measurements. EPR spectra of a powder specimen of **2** were recorded on a Bruker ESP300E X-band (9.7 GHz) spectrometer at room temperature.

UV–Vis–NIR Measurements. UV–vis–NIR spectra of **2** in Nujol were recorded on a Hitachi U3400 spectrometer (300–3200 nm) at room temperature.

Acknowledgment. This work was supported by a Grant-in-Aid for Scientific Research (No. 19550135) from the Ministry of Education, Culture, Sports, Science and Technology, Japan, and by a research grant from the Japan Securities Scholarship Foundation. The authors thank Ms. Mio Ishida (Mitsubishi Chemical Corp.) for technical support in the UV–vis–NIR spectroscopic measurements.

Supporting Information Available: CIF files including selected geometrical parameter tables for **1** and **2**. This material is available free of charge via the Internet at <http://pubs.acs.org>.

IC8020589